JOURNAL OF BACTERIOLOGY, Sept. 2006, p. 6298–6307 Vol. 188, No. 17
0021-9193/06/$08.00+0 doi:10.1128/JB.00334-06

PBP5 Complementation of a PBP3 Deficiency in *Enterococcus hirae*†

S. Leimanis,[1] N. Hoyez,[1] S. Hubert,[1] M. Laschet,[1] Eric Sauvage,[1] R. Brasseur,[2] and J. Coyette[1]*

Centre d'Ingénierie des Protéines, Université de Liège, Institut de Chimie, B6, B-4000 Liège, Belgium,[1] and Centre de Biophysique Moléculaire Numérique, Faculté Universitaire des Sciences Agronomiques, Gembloux, Belgium[2]

Received 7 March 2006/Accepted 9 June 2006

The low susceptibility of enterococci to β-lactams is due to the activity of the low-affinity penicillin-binding protein 5 (PBP5). One important feature of PBP5 is its ability to substitute for most, if not all, penicillin-binding proteins when they are inhibited. That substitution activity was analyzed in *Enterococcus hirae* SL2, a mutant whose *pbp5* gene was interrupted by the *nisRK* genes and whose PBP3 synthesis was submitted to nisin induction. Noninduced SL2 cells were unable to divide except when plasmid-borne *pbp5* genes were present, provided that the PBP5 active site was functional. Potential protein-protein interaction sites of the PBP5 N-terminal module were mutagenized by site-directed mutagenesis. The T_{167}-L_{184} region (designated site D) appeared to be an essential intramolecular site needed for the stability of the protein. Mutations made in the two globular domains present in the N-terminal module indicated that they were needed for the suppletive activity. The P_{197}-N_{209} segment (site E) in one of these domains seemed to be particularly important, as single and double mutations reduced or almost completely abolished, respectively, the action of PBP5.

Cell morphology in eubacteria is determined mainly by the peptidoglycan layer that is synthesized by a battery of cytoplasmic and membrane-bound enzymes, among which are the DD-peptidases (26, 42, 61). These peptidases, commonly designated penicillin-binding proteins (PBPs), are serine-active enzymes that belong to a large family of penicillin-recognizing proteins whose active sites contain three conserved motifs. Generally, the PBPs lose their DD-peptidase activity by forming a long-lived covalent bond with penicillins (26).

The PBPs are separated into two large groups on the basis of their sizes. The low-molecular-mass proteins are essentially monomodular DD-peptidases that have been shown to play a morphogenetic role in *Escherichia coli* as well as in *Streptococcus pneumoniae* cells (11, 12, 41, 43, 66). In contrast, the high-molecular-mass PBPs are essential bimodular enzymes that bind penicillins on their C-terminal module. They are further subdivided into two classes. Class A PBPs have an N-terminal module acting as a glycosyltransferase and are characterized by the presence of five typical conserved amino acid motifs. Class B PBPs possess three conserved amino acid motifs in their N-terminal modules that have no detectable enzymatic activity but seem, however, to be essential for cell morphogenesis (26).

Different observations suggest that rod-shaped bacteria possess two morphogenetic systems, one responsible for cell elongation and the other responsible for cytokinesis (50, 52). For example, separate inactivation of *E. coli* class B PBP2 and PBP3 either by β-lactam antibiotics or by mutagenesis shows that the first is specifically required for cell elongation and that the second is required for cell division (4, 59). In addition, two protein complexes containing different PBPs could be isolated from *Haemophilus influenzae* and *Bacillus subtilis* cells (1, 58).

Consistent with their function, PBP3 of *E. coli* (38, 63, 65) or PBP2b and PBP1 of *Bacillus subtilis* (54) localize in the area of developing septa and of completed poles. These PBPs are part of a multiprotein-synthesizing machinery, designated the divisome (6, 21, 42, 54), whose assembly has been studied by different approaches (16, 31, 38, 45, 63).

The composition of the multiprotein complex needed for cell elongation is not yet well documented, but it is thought to be structurally analogous to the divisome (30). In addition to *pbpA*, encoding PBP2, other different genes such as *rodA* (59, 60) and *mreBCD* (33, 54, 60) are required for elongation in *E. coli*.

Morphogenesis of cocci was thought to be relatively simple, with most of the cell wall synthesis taking place at the site of septum formation (25, 28). However, on the basis of the inhibition of cell division by antibiotics or by thermosensitive mutations, it was proposed that they be separated into two groups: those that possess a site for septum formation only and those that in addition have a site for lateral wall elongation that would be less effective than that in rod-shaped cells (35, 52). *Staphylococcus aureus* is probably a member of the first group, as cell wall synthesis appears to occur only at the division site (48).

The low susceptibility of enterococci to β-lactams is due to the activity of a low-affinity class B PBP, designated PBP5 (23, 64). In the presence of antibiotic concentrations that inhibit all the PBPs except PBP5, enterococci continue to multiply (22). Under these conditions, even in highly resistant strains, PBP5 maintains sufficient transpeptidase activity to synthesize a normal peptidoglycan in *Enterococcus faecium* and *Enterococcus hirae* (7, 55, 67). When grown in the presence of sub-MIC concentrations, the penicillin-resistant *Enterococcus faecalis* strain 56R has a slightly less cross-linked peptidoglycan with fewer oligomers but more dimers than the wild type (56). Note that when PBP5 is the only active DD-transpeptidase, these cells also need the help of an active glycosyltransferase to synthesize peptidoglycan, as class B PBPs were shown to be unable to polymerize glycan strands (26, 49).

Different morphological observations of β-lactam-treated enterococcal cells indicate that they should have two cell wall-

* Corresponding author. Mailing address: Centre d'Ingénierie des Protéines, Université de Liège, Institut de Chimie, B6, B-4000 Liège, Belgium. Phone: 32 4 3663399. Fax: 32 4 3663364. E-mail: jcoyette@ulg.ac.be.

† Supplemental material for this article may be found at http://jb.asm.org/.

synthesizing machineries (52). Treatment of *E. hirae* ATCC 9790 with ampicillin or cephalotin concentrations that have little effect on the increase in cell growth but that result in a relatively strong inhibition of cell division lead to a doubling of average volumes and lengths of the cells during a 60-min period (29). Under these conditions, on the basis of 50% inhibitory concentrations, all the PBPs except PBP5 should be saturated (9).

Exponential-phase cells of *E. hirae* ATCC 9790 treated with low concentrations of cefotaxime ($\leq 0.25 \times$ MIC) form bloated rods in which septa are initiated but not formed as a result of the specific inhibition of class B PBP2 and PBP3 (10). It was also shown that when thermosensitive PBP3 *E. hirae* mutants constitutively overproduce PBP5, they grow normally at the nonpermissive temperature (8). This again indicates that PBP5 can compensate for the lack of PBP3 that is determined by a gene located in the *dcw* cluster devoted to cell division (17). Presumably, like in other bacteria (42, 62), when PBP3 is specifically inhibited, the divisome is inactivated, and the cells continue to build their peptidoglycan with their peripheral wall-synthesizing complex. One may suppose that to be able to fulfill its suppletive activity in *E. hirae*, PBP5 is integrated into the divisome with PBP3 or into a multiprotein biosynthetic machinery that has similar functions.

In this study, we modified *E. hirae* cells to place PBP3 synthesis under the control of the *nisAp* promoter that is strongly repressed in the "nisin-controlled expression" (NICE) system that was successfully used to analyze the expression of different genes in various gram-positive bacteria (15, 46). Our results indicate that for several hours, noninduced recombinant cells do not produce PBP3, stop dividing, and elongate. However, if PBP5 is synthesized, these cells divide normally in spite of the absence of PBP3. In parallel, examination of the N-terminal-domain sequence of PBP5 with a predictive method that was used to establish the functionality of different regions of *E. coli* PBP3 and FtsW led to the identification of potential protein-protein interacting segments (24, 38, 47). Some residues in these segments were modified by site-directed mutagenesis. One residue appeared to be crucial to maintain the stability of PBP5, and another seemed to be more specifically required for its suppletive activity in noninduced cells.

MATERIALS AND METHODS

Bacterial strains, media, growth conditions, and MIC determinations. The *E. coli* and *E. hirae* strains used in this work are listed in Table 1. *E. coli* strains were grown in Luria broth (LB) at 37°C. *E. hirae* strains were grown in either M17 medium to prepare electrocompetent cells (51) or brain heart infusion (BHI) broth at 37°C or at 28° and 42°C when homologous recombinants were isolated. Growth curves were established by measuring the absorbance at 550 nm (A_{550}) or by determining cell numbers on plates at regular intervals. The media were supplemented with ampicillin (100 μg/ml) (Bristol-Myers Squibb, Brussels, Belgium), kanamycin (100 μg/ml) (Calbiochem, Bierges, Belgium), chloramphenicol (10 μg/ml), erythromycin (5 or 10 μg/ml) (both from Fluka, Bornem, Belgium), and benzylpenicillin (PenG) (0.1 μg/ml) (Aventis, Lyon, France) as indicated. Other selective additives such as 5-bromo-4-chloro-3-indolyl-β-D-galactopyranoside (X-Gal) (40 μg/ml), isopropyl-β-D-thiogalactopyranoside (IPTG) (7 μg/ml) (both from Immunosource, Zoersel-Halle, Belgium), and 5-bromo-4-chloro-3-indolyl-glucuronide (X-Gluc) (0.5 mM) (Research Organics Inc., Cleveland, Ohio) were used or applied to the media as required. MICs were determined in 1 ml of BHI broth in 24-well culture plates, in at least three independent determinations, essentially as previously described (51).

Plasmid constructions. Common *E. coli* plasmids (Table 1) were used for cloning purposes. Gene disruption or replacement experiments were carried out by using the pER924 shuttle vector as previously described (51).

(i) pDML1615. A 2.2-kb *pbp3* fragment was amplified by PCR by using the DNA of ATCC 9790 as a template and primers SELpbp3BamHI and SELpbp3SacI (Table 2). These oligonucleotides were designed to place a BamHI site just upstream of the *pbp3* ATG codon and a SacI site just downstream of the stop codon, respectively. The *pbp3* fragment was cloned into pUC18, which was used as an intermediate, since for unknown reasons, direct cloning into pNZ8020 was unsuccessful. The *pbp3* gene was then transferred into pNZ8020 under the dependence of the *nisAp* promoter (*nisAp-pbp3* fusion) to generate pDML1615.

(ii) pDML1621. A 3.6-kb chromosomal DNA fragment of *E. hirae* SL1, which contained the entire *pbp3* gene as well as the upstream *mraW* and *ftsL* and downstream *mraY* genes, was amplified by PCR by using primers MFPMupBamHI and MFPMlowEcoRI (Table 2) and cloned into BamHI- and EcoRI-digested pUC18 to obtain pDML1616 (see the supplemental material).

By digestion with BamHI and KpnI (the KpnI site is present in the last quarter of *pbp3*), the pDML1616 insert was reduced to 2.6 kb and cloned into pUC18 to generate pDML1617, where it was mutagenized to introduce an NcoI restriction site at the level of the starting ATG codon of *pbp3* (NcoIup and NcoIlow primers) (Table 2) by site-directed mutagenesis. That new plasmid, containing both the *mraW* and *ftsL* genes as well as a large part of *pbp3* (designated below as *pbp3a*), was named pDML1618.

In parallel, the 0.8-kb kanamycin resistance cassette (*aph3′* or Km^r gene) present in pDG792 was amplified by PCR by using primers KANup-NcoI and KANlow-KpnI (Table 2) (the NcoI site overlapped the Km^r gene starting ATG codon), cloned into the pGEM-T Easy vector, digested by the NcoI and KpnI enzymes, and finally substituted into pDML1618 for the 1.6-kb *pbp3a* fragment. The resulting plasmid, pDML1619, was then digested by the BamHI and KpnI restriction enzymes to isolate the 1.8-kb *mraW-ftsL*-Km^r fragment that was introduced into pDML1616 as a substitute for the 2.6-kb *mraW-ftsL-pbp3a* fragment. The resulting plasmid, pDML1620, thus contained the *mraW-ftsL*-Km^r*-pbp3b-mraY* genes (*pbp3b* corresponds to the terminal end of *pbp3*) that were finally excised by BamHI and EcoRI digestion and cloned into the thermosensitive shuttle vector pER924 to obtain pDML1621 (see the supplemental material).

(iii) pDML1626 and pDML1627 to pDML1633. The 2.6-kb *pbp5* insert of pDML546 was cloned into pBR322 at the SalI and EcoRI sites to yield pDML1626. When fused at the EcoRI site of pIL253, it produced the *E. coli*/*E. hirae* shuttle vector pDML1627. Plasmids pDML1628 to pDML1633 were the result of similar fusions with the different pDML1626 mutants.

(iv) pDML2230 and pDML2231. Two plasmids carrying the *pbp5* gene of *E. faecium* ($pbp5_{Efm}$) with its promoter and terminator sequences were constructed with the 2.2-kb PCR fragment amplified from pDML517 with primers ON1 and ON2*, which were designed to introduce the EcoRI and BamHI sites at each end, respectively. That 2.2-kb PCR fragment was cloned into pBR322 to yield pDML1699, which was then fused to pIL253 to generate pDML2330. It was also inserted into vector pUC18del that was obtained after the removal of AatII-XbaI from pUC18. Plasmid pDML1698, thereby obtained, was used to mutagenize the Ser422 residue and then construct the pDML2231 shuttle vector.

Construction of the *E. hirae pbp5*::*nisRK* SL1 strain. A 2.4-kb blunt-ended HpaII-PstI DNA fragment that contained the complete *nisRK* operon was isolated from plasmid pNZ9500 and inserted into the blunt-ended SstI site (position 1144 from the *pbp5* ATG codon) inside the 1.6-kb *pbp5* fragment of pDML1600 to generate pDML539. The 4-kb EcoRI-BamHI *pbp5*::*nisRK* fragment isolated from pDML539 was cloned into the thermosensitive pER924 shuttle vector to construct the integrative plasmid pDML1614, which was used to electroporate *E. hirae* ATCC 9790 cells and to isolate, as previously described (51), *pbp5*-negative double recombinants appearing on plates as penicillin-sensitive *pbp5*-negative colonies.

The susceptibility of these *pbp5*-negative clones, verified by measuring the penicillin MIC, as expected, was 40 times higher (MIC = 0.015 μg/ml) than that of the parental strain (0.6 μg/ml) (51). Integration of the *nisRK* gene cluster into *pbp5* was also verified by PCR by using both pbp5 4546 and pbp5 B4 primers (Table 2), which hybridized upstream and downstream, respectively, of the insertion point in *pbp5*. The PCR fragments obtained from the recombinants were 2.4 kb longer (4.7 kb) than those obtained from ATCC 9790 (2.3 kb), indicating that the *nisRK* fragment had been inserted (results not shown). Membranes of a randomly picked *pbp5*::*nisRK* recombinant, designated SL1, were prepared, labeled with [^{14}C]PenG, and compared with those of ATCC 9790 and the penicillin-resistant strain R40, which overproduces PBP5. As expected, SL1 did not synthesize PBP5 (Fig. 1A).

General DNA methods. Standard DNA methodologies were used (2). DNA fragments, PCR products, plasmids, and the genomic DNA of *Enterococcus* cells

TABLE 1. Strains and plasmids used in this study

Strain or plasmid	Genotype and/or phenotype[a]	Source or reference
Strains		
E. coli		
Top10F′	F′ [*lacI*^{q} Tn*10* (Tet^r)] *mcrA* Δ(*mrr-hsdRMS-mcrBC*) ϕ80 *lacZ*Δ*M15* Δ*lacX74 deoR recA1 araD139* Δ(*ara-leu*)*7697 galU galK rpsL*(Str^r) *endA1 nupG*	Invitrogen
DH5α	F$^-$ *endA1 hsdR17*(r_K^- m_K^+) *glnV44 thi-1 recA1 gyrA*(NaI^r) *relA1* Δ(*lacIZYA-argF*)*U169 deoR* ϕ80d*lacZ*Δ(*lacZ*)*M15*	Invitrogen
E. hirae		
ATCC 9790	Wild-type strain (MIC of PenG, 0.6 μg/ml)	ATCC[b] collection
R40	Pen^r mutant derived from ATCC 9790 (MIC of PenG, 60 μg/ml)	22
SL1	ATCC 9790 *pbp5*::*nisRK* (MIC of PenG, 0.015 μg/ml)	This study
SL2	SL1 *pbp3* negative/pDML1615	This study
Plasmids		
pBR322	*E. coli* cloning vector	Amersham Pharmacia Biotech
pDG792	*E. coli* vector carrying the 1.5-kb *aph3′* (Km^r) gene cassette	27
pER924	*E. coli*/gram-positive shuttle vector (Ts *ori*$^+$)	3
pGEM-T Easy	*E. coli* cloning vector for PCR products	Promega
pIL253	Erm^r high-copy-number gram-positive cloning vector	57
pSL1190	*lacZ E. coli* phagemid	Amersham Pharmacia Biotech
pUC18	*lacZ E. coli* cloning vector	Amersham Pharmacia Biotech
pNZ8008	Cm^r pNZ273 carrying the *nisAp-gusA* reporter gene, gram-positive/gram-negative origin	13
pNZ8020	Cm^r pNZ8008 without *gusA*	14
pNZ9500	pUC19ery carrying the 3′ end of *nisP* and *nisRK* genes of *Lactococcus lactis* NZ9700 (2.7-kb DNA fragment)	32
pDML517	pBR322 carrying the $pbp5_{Efm}$ gene of *E. faecium* D63^r (7.7-kb EcoRI fragment)	67
pDML539	pDML1600 carrying the *pbp5*::*nisRK* genes	This study
pDML540	pBR322 carrying the *ftsW psr pbp5* genes of *E. hirae* R40 (6.9-kb EcoRI fragment)	20
pDML541	pBR322 carrying the *pbp5* gene (2.6-kb EcoRI/PvuI fragment derived from pDML540)	40
pDML545	pET22b$^+$ (Km^r) carrying the truncated NcoI-NotI PCR fragment of *pbp5* (94 to 2,036 bp) of *E. hirae* R40	44
pDML546	pUC18 carrying the *pbp5* gene (2.6-kb EcoRI-SalI fragment derived from pDML541)	40
pDML1600	pUC18 carrying the *pbp5* gene (1.6-kb PCR fragment)	51
pDML1614	pER924 carrying the *pbp5*::*nisRK* genes (EcoRI/BamHI insert of pDML539)	This study
pDML1615	pNZ8020 carrying the *nisAp-pbp3* (*pbp3i*) gene	This study
pDML1616	pUC18 carrying the *mraW-ftsL-pbp3-mraY* genes (3.6-kb BamHI-EcoRI fragment of ATCC 9790)	This study
pDML1617	pUC18 carrying the *mraW-ftsL-pbp3a* genes (BamHI-KpnI fragment of pDML1616)	This study
pDML1618	pDML1617 with an additional NcoI restriction site at the *pbp3a* starting codon	This study
pDML1619	pDML1617 carrying the *mraW-ftsL*-Km^r genes	This study
pDML1620	pDML1616 carrying the *mraW-ftsL*-Km^r-*pbp3b-mraY* fragment	This study
pDML1621	pER924 carrying the *mraW-ftsL*-Km^r-*pbp3b-mraY* fragment of pDML1621	This study
pDML1623	pUC18 carrying the 270-bp HindIII-PstI *pbp5* fragment encoding the D and E sites	This study
pDML1626	pBR322 carrying the wild-type or mutated *pbp5* genes (EcoRI-SalI fragment of pDML541)	This study
pDML1627	pIL253/pDML1626 fusion carrying *pbp5*	This study
pDML1628	pDML1627 carrying the *pbp5*(*K172N*/*R173N*) gene (M1 mutant)	This study
pDML1629	pDML1627 carrying the *pbp5*(*K199Q*/*K203Q*) gene (M2 mutant)	This study
pDML1630	pDML1627 carrying the *pbp5*(*K203Q*) gene (M3 mutant)	This study
pDML1631	pDML1627 carrying the *pbp5*(*5K-S*) gene (M4 mutant)	This study
pDML1632	pDML1627 carrying the *pbp5*(*R173N*) gene (M5 mutant)	This study
pDML1633	pDML1627 carrying the *pbp5*(*K199Q*) gene (M6 mutant)	This study
pDML1697	pSL1190 carrying the 5′-end 390-bp NcoI-SpeI fragment of *pbp5* isolated from pDML545	This study
pDML1698	pUC18 derived, carrying the $pbp5_{Efm}$ gene (2.2-kb EcoRI-BamHI fragment of *E. faecium* D63^r)	This study
pDML1699	pBR322 carrying the $pbp5_{Efm}$ gene (2.2-kb EcoRI-BamHI fragment of *E. faecium* D63^r)	This study
pDML2330	pIL253/pDML1699 fusion carrying $pbp5_{Efm}$	This study
pDML2331	pDML2330 carrying $pbp5_{Efm}$(*S422A*)	This study

[a] Cm^r, chloramphenicol resistant; Erm^r, erythromycin resistant; Km^r, kanamycin resistant; Pen^r, penicillin resistant.
[b] ATCC, American Type Culture Collection.

(collected at the end of the exponential phase) were purified as previously reported (36, 51). *E. hirae* plasmids were isolated from protoplasts prepared from cells at the end of the exponential phase that were lysed for 30 min at 37°C with lysozyme (3 mg/ml) in a solution containing 10 mM Tris, 1 mM EDTA, and 27% (wt/vol) sucrose (pH 8) and collected by low-speed centrifugation (3,000 rpm for 3 min). Nucleotide sequencing was performed as previously described (51), with Cy5 primers identical to some of those shown in Table 2. Restriction endonucleases from Promega (Leiden, The Netherlands), Life Technologies (Merelbeke,

TABLE 2. Oligonucleotides used in this study

Oligonucleotide[b]	Sequence[a]	Gene
pbp5 4546	5′-TAAGAAAATGTGAGCGGAGGG-3′	*pbp5*
pbp5 B4*	5′-TCAGGATTCACAGCAAATAGGAAGC-3′	*pbp5*
SELpbp3BamHI	5′-GGG**GGATCC**AAATGAGTCTTAAAAATA-3′	*pbp3*
SELpbp3SacI*	5′-GAA**GAGCTC**TCTCTCCCAATTCTATTCTTA-3′	*pbp3*
MFPMupBamHI	5′-GATATGCGTAT**GGATCC**ATCAGCACCTCTG-3′	*mraY-ftsL-pbp3-mraW*
MFPMlowEcoRI	5′-CGTACCAGGATA**GAATTC**TGAACGATAGAC-3′	*mraY-ftsL-pbp3-mraW*
KANAupNcoI	5′-GAAATAAT**CCATGG**CTAAAATGAGAATATC-3′	*aph3′*
KANAlowKpnI*	5′-CTCCTC**GGTACC**ACTAAAACAATTCATCCAGTAAAATATAATA-3′	*aph3′*
NcoI-up	5′-GAAAGTGAAGT**CCATGG**GTCTTAAAAATAAATTC-3′	*pbp3*
NcoI-low*	5′-GAATTTATTTTTAAGAC**CCATGG**ACTTCACTTTC-3′	*pbp3*
O5M1a	5′-ACTAGTGAGGAAGCT-AAC-AAC-GGCGATATCCTT-3′	*pbp5*
O5M1b*	5′-AAGGATATCGCC-GTT-GTT-AGCTTCCTCACTAGT-3′	*pbp5*
O5M2a	5′-ATCGTTCCTAGA-CAG-CTGGGAGAA-CAA-GAAGAGAAAACA-3′	*pbp5*
O5M2b*	5′-TGTTTTCTCTTC-TTG-TTCTCCCAG-CTG-TCTAGGAACGAT-3′	*pbp5*
O5M3a	5′-AAGCTGGGAGAA-CAA-GAAGAGAAAACA-3′	*pbp5*
O5M3b*	5′-TGTTTTCTCTTC-TTG-TTCTCCCAGCTT-3′	*pbp5*
O5M5a	5′-GAGGAAGCTAAA-AAC-GGCGATATCCTT-3′	*pbp5*
O5M5b*	5′-AAGGATATCGCC-GTT-TTTAGCTTCCTC-3′	*pbp5*
O5M6a	5′-ATCGTTCCTAGA-CAG-CTGGGAGAAAAA-3′	*pbp5*
O5M6b*	5′-TTTTTCTCCCAG-CTG-TCTAGGAACGAT-3′	*pbp5*
ON6	5′-TATGCCCCTGGAGCGACGTTTAAAATGATC-3′	*pbp5*
ON7*	5′-GATCATTTTAAACGTCGCTCCAGGGGCATA-3′	*pbp5*
O1K75K76	5′-CATTCACAGACTAGCAGCACAATTTCTGAA-3′	*pbp5*
O1K75K76*	5′-TTCAGAAATTGTGCTGCTAGTCTGTGAATG-3′	*pbp5*
O2K108K109	5′-ATTTAAAAGTGACGAGCAGCGATAGTGAAACCTATT-3′	*pbp5*
O2K108K109*	5′-AATAGGTTTCACTATCGCTGCTCGTCACTTTTAAAT-3′	*pbp5*
O3K146	5′-AATGATCAGATCAGCATCAACTGGCAG-3′	*pbp5*
O3K146*	5′-CTGCCAGTTGATGCTGATCTGATCATT-3′	*pbp5*
UP	5′-GTAAAACGACGGCCAGT-3′	M13 universal sequencing
RP	5′-CAGGAAACAGCTATGAC-3′	M13 reverse sequencing

[a] Boldface type indicates the BamHI, SacI, EcoRI, KpnI, and NcoI restrictions sites, and underlined sequences correspond to modified codons.
[b] *, complementary.

Belgium), and Fermentas (St. Leon-Rot, Germany); calf intestinal alkaline phosphatase from Roche Diagnostics (Brussels, Belgium); T4 DNA polymerase from Life Technologies (Merelbeke, Belgium); and T4 DNA ligase from Boehringer Ingelheim Bioproducts (Verviers, Belgium) were used as recommended by the suppliers.

PCR. PCR amplifications were performed in a TRIO-Thermoblock Biometra thermocycler (Eurogentec, Liège, Belgium) with primers obtained from either Amersham Pharmacia Biotech or Eurogentec (Table 2). The *Taq*, *Pwo*, Vent, and Biotools DNA polymerases from Amersham Pharmacia Biotech, Eurogentec, New England Biolabs (Westburg, Leusden, The Netherlands), and Labsystem (Brussels, Belgium), respectively, were used according to the manufacturers' recommendations. Amplifications were usually carried out as previously described (51).

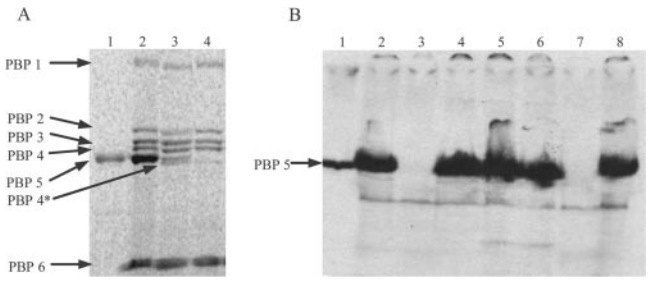

FIG. 1. SDS-PAGE and fluorogram of the membrane-bound PBPs of different *E. hirae* strains. (A) Membranes were labeled for 60 min with 100 μM [^{14}C]PenG. Lane 1, purified soluble PBP5; lane 2, R40; lane 3, ATCC 9790; lane 4, SL1. (B) Membranes (pretreated for 15 min with 10 μM nonradioactive PenG) were incubated for 60 min with 100 μM [^{14}C]PenG for specific labeling of $PBP5_{Eh}$. Lane 1, purified soluble $PBP5_{Efm}$; lane 2, SL1/*pbp5*$_{Eh}$; lane 3, SL1/*pbp5*(*K172N*/*R173N*); lane 4, SL1/*pbp5*(*K199Q*/*K203Q*); lane 5, SL1/*pbp5*(*K203Q*); lane 6, SL1/*pbp5*(*5K-S*); lane 7, SL1/*pbp5*(*R173N*); lane 8, SL1/*pbp5*(*K199Q*).

Directed mutagenesis. The site-directed mutagenesis of *pbp5* was performed with the QuickChange site-directed mutagenesis kit (Stratagene Europe, Amsterdam, The Netherlands) on a 270-bp fragment encoding the S_{125}-A_{215} peptide of PBP5 that was excised from pDML541 by a double HindIII and PstI digestion and cloned into pUC18 to generate pDML1623. Primer pairs O5M1a/O5M1b, O5M2a/O5M2b, O5M3a/O5M3b, O5M5a/O5M5b, and O5M6a/O5M6b (Table 2) were used to produce the $K_{172}N/R_{173}N$ (M1 mutant), $K_{199}Q/K_{203}Q$ (M2 mutant), $K_{203}Q$ (M3 mutant), $R_{173}N$ (M5 mutant), and $K_{199}Q$ (M6 mutant) substitutions, respectively. The resulting plasmids were named pDML1623M1, pDML1623M2, pDML1623M3, pDML1623M5, and pDML1623M6, respectively. The HindIII-PstI fragments carrying the different mutations were then exchanged with the corresponding fragment of pDML1626 to obtain pDML1626M1, pDML1626M2, pDML1626M3, pDML1626M5, and pDML1626M6, respectively.

To introduce the five K-to-S substitutions in the N-terminal end of PBP5, a 390-bp NcoI-SpeI fragment was isolated from pDML545 and cloned into pSL1190 to generate pDML1697. The construct was then mutagenized in three successive steps with three pairs of primers, O1K75K76/O1K75K76*, O2K108K109/O2K108K109*, and O3K146/O3K146* (Table 2). The final mutated fragment was then exchanged with the corresponding wild-type fragment of pDML541 by a double ScaI-SpeI digestion. The ScaI site is present 60 bp downstream of the NcoI site. Finally, the mutated *pbp5* gene was introduced into pDML1626 by exchange of the EcoRI-SalI fragment to generate pDML1626M4.

The S422A substitution of $PBP5_{Efm}$ was made in pDML1698 by site-directed mutagenesis with the ON6 and ON7* primers. The AccI fragment isolated from the $S_{422}A$ *pbp5*$_{Efm}$ [*pbp5*$_{Efm}$(*S422A*)] gene was then exchanged with that of pDML1699 to generate pDML1699S_{422}A, which was fused to pIL253 at the EcoRI site to yield pDML2331.

Transformation of *E. hirae* cells and isolation of recombinants. *E. coli* competent cells and *E. hirae* electrocompetent cells were transformed as previously described (2, 51). Gene disruptions or deletions in *E. hirae* cells were achieved by

double recombination of electroporated integration vectors as previously described (5, 51).

PBP detection by radioactive labeling and immunoblotting. PBP profiles were established with cells that were collected at an A_{550} of 1.0. Preparation of membranes of the different *E. hirae* clones, estimation of protein contents, [^{14}C]PenG labeling, sodium dodecyl sulfate-polyacrylamide gel electrophoresis (SDS-PAGE), and fluorography of PBPs were performed as described elsewhere previously (67). Except when stated otherwise, 200-μg protein samples were used. Modification of the fluorography procedure, detection of labeled PBPs, and Western blot analysis with anti-PBP5 rabbit polyclonal antibodies were previously described (51). The truncated soluble PBP5$_{Efm}$ used as a control in some of these procedures was obtained as previously described (53).

β-Glucuronidase activity. Nisin was obtained from Sigma as a 2.5% solution in sodium chloride containing denatured milk proteins. Stock solutions of nisin were made by suspending 10 mg of the nisin mixture per ml of 0.05% acetic acid and then diluting the preparation (10-fold) with dimethyl sulfoxide. These stock solutions were stored at −20°C. Further dilutions were made with water and were used immediately.

For quantitative β-glucuronidase assay, *E. hirae* cells were grown up to an A_{550} of 0.5, induced with different nisin concentrations, grown for another 90 min, and harvested. After being resuspended in 50 mM $NaHPO_4$ buffer (pH 7) to a final A_{600} of 2.0, these cells were permeabilized and used immediately for the glucuronidase assay in the presence of 100 mM *para*-nitrophenyl-β-D-glucuronic acid (Clontech Laboratories, Inc., Palo Alto, Calif.) as previously described (34).

Prediction of interaction sites. In the method used here, a 7- or 11-amino-acid segment is moved along the primary structure of a protein one residue at a time. For the central residue of each segment, a mean hydrophobicity, <H>, value and a mean hydrophobic moment, <μ>, value were calculated. Both values characterizing each residue were plotted (18, 19, 24). It has been determined that different putative sites possess one or several residues for which <H> values are smaller than −0.5 and <μ> values are greater than 0.5. Replacements of one residue that in principle do not modify the secondary and tertiary structures may affect the predicted amphiphilicity. Those that have the strongest influence on that property could greatly change the putative interacting capacity of a site.

RESULTS

Testing of the NICE system and the *trans* expression of *pbp5* and *pbp3* in *E. hirae* SL1. To be fully functional, the NICE system requires the presence and activity of the *nisRK* genes that signal the presence of nisin (the inducer) and activate genes placed under the control of the *nisA* promoter (*nisAp*). The two *nisRK* genes were thus first inserted into the *pbp5* gene that was shown to be dispensable in *E. hirae* ATCC 9790 (51). The thereby constructed PBP5-deficient clone, SL1, was also needed to assess the activity of PBP5 variants.

As expected, in the presence of nisin, SL1/pNZ8008 transformants appeared as blue colonies on plates containing X-Gluc but remained uncolored if noninduced. Induction of the glucuronidase activity by the *nisAp-gusA* gene was also followed by measuring the rate of hydrolysis of the *p*-nitrophenyl-β-D-glucuronide substrate in permeabilized cells. The activity was detectable at very low concentrations of nisin (10 ng/ml) and presented, as previously shown (34), a good linear dose-response relationship up to concentrations just below the MIC (nisin MIC = 5 μg/ml). The activity of noninduced SL1/pNZ8008 cells remained under the limits of detection. The NICE system was thus functional in *E. hirae*. It is important that in spite of the presence of nisin (0.25 μg/ml), the growth rates of either ATCC 9790 and SL1 or SL1/pNZ8008 (~29-min and ~32-min generation times, respectively) were not modified.

Expression of *pbp5$_{Eh}$*. The 11-kb pDML1627 shuttle vector carrying wild-type *E. hirae pbp5* (*pbp5$_{Eh}$*) was used to test the *trans* expression of *pbp5$_{Eh}$*. As shown by SDS-PAGE and fluorography, radioactively labeled membranes of SL1/pDML1627 clones designated below as SL1/*pbp5$_{Eh}$*, grown in the presence of erythromycin, synthesized relatively large amounts of active PBP5$_{Eh}$ (Fig. 1B, lane 2). As expected, the resistance of SL1/*pbp5$_{Eh}$* cells to PenG was much increased (MIC = 20 μg/ml) compared to that of the parental SL1 strain. The PBP5$_{Eh}$ produced in SL1 was thus functional.

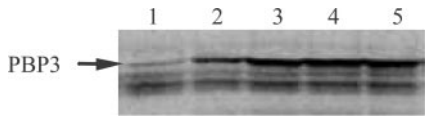

FIG. 2. SDS-PAGE and fluorogram of the 77-kDa membrane-bound PBP3 of nisin-induced SL1/*pbp3i* cells. Lane 1, noninduced cells; lanes 2 to 5, nisin-induced cells (10, 20, 40, and 80 ng/ml, respectively). Membranes (500 μg) were labeled for 10 min with 100 μM [^{14}C]PenG. Part of the gel shows PBPs 2 to 4. Under these conditions, PBP2 was barely visible.

Expression of the *nisAp-pbp3* fusion. To assess the ability of native and mutant forms of PBP5$_{Eh}$ to substitute for PBP3, we needed a strain whose PBP3 synthesis could be controlled. We chose to inactivate the chromosomal gene in the presence of the inducible *nisAp-pbp3* gene fusion carried on the pDML1615 plasmid. However, the expression of that fusion had to first be tested.

Induced PBP3 synthesis in SL1/pDML1615 transformants, designated below as SL1/*pbp3i*, progressively increased with increasing nisin concentrations of up to 2 μg/ml (Fig. 2). Synthesis of PBP3 in noninduced SL1/*pbp3i* remained weak and was most probably due to the chromosomal gene that is still present. It is important that neither the growth nor the morphology appeared to be changed in *E. hirae* SL1/*pbp3i* cells producing large amounts of PBP3.

Isolation of SL2, a *pbp3*-conditional derivative of SL1. Inactivation of the chromosomal *pbp3* gene was performed in SL1/*pbp3i* cells transformed with the integrative pDML1621 vector. Nisin (0.5 μg/ml) and chloramphenicol (10 μg/ml) were added to the medium at all steps to produce enough PBP3 in the absence of the chromosomal *pbp3* and to maintain pDML1615, respectively. However, no kanamycin-resistant colonies were found. Double *pbp3*-deficient recombinants could nevertheless be differentiated, as in the absence of nisin, they formed colonies much later (minimum of 2 days) than parental SL1/*pbp3i* cells. One randomly picked *pbp3*-deficient SL1/*pbp3i* recombinant was named SL2.

PCRs were used to verify the integration of the 0.8-kb kanamycin cassette. It was amplified by using primers KANup-NcoI and KANlow-KpnI (Table 2) from SL2 cells but not from SL1 cells. In addition, PCR fragments obtained from pDML1616 and SL1 (two *pbp3* controls) were 0.8 kb longer than those (2.8 kb) obtained from pDML1621 and SL2 when primers MFPMupBamHI and MFPMlowEcoRI (Table 2), which hybridized at both ends of the *mraW-ftsL-pbp3-mraY* locus, were used (data not shown). That difference was in good accordance with the replacement of the PBP3a fragment by the Km^r cassette.

One could explain the lack of kanamycin resistance of the recombinants by either a lack of activity of the Km^r gene or, more probably, an insufficient expression of the Km^r gene due to a *pbp3* promoter that was too weak. As the recombinants grew normally,

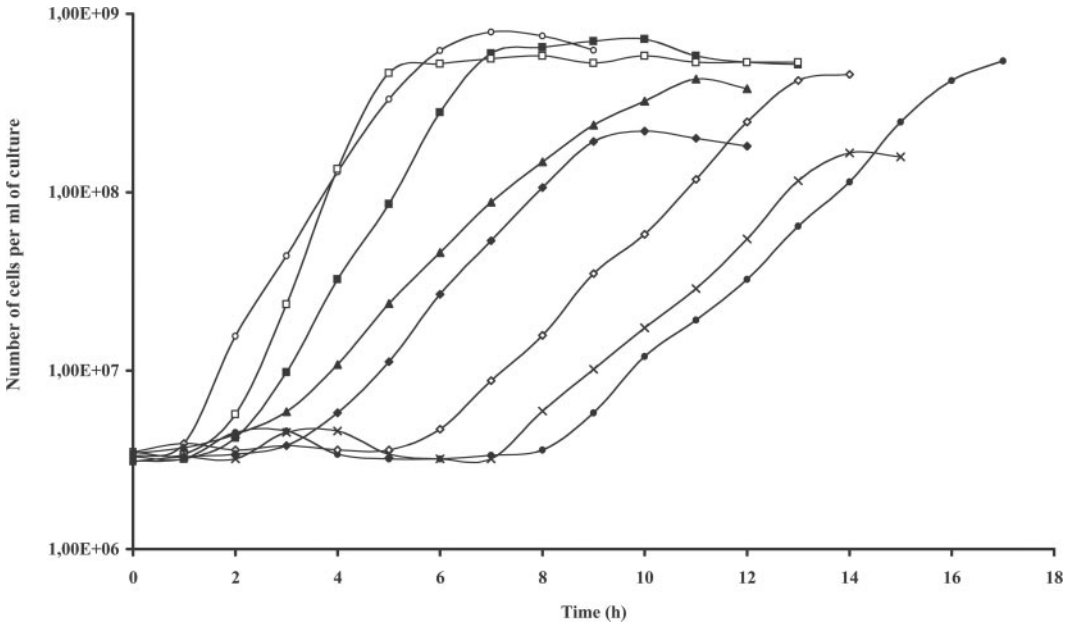

FIG. 3. Growth curves of SL2 cells (cell counts) transformed with wild-type and mutated $pbp5_{Eh}$ genes. Mean values of four to six independent cultures were used. Shown are induced (○) and noninduced (●) SL2, induced (□) and noninduced (■) SL2/$pbp5_{Eh}$, noninduced SL2/*pbp5*(*K199Q*/*K203Q*) (×), SL2/*pbp5*(*K203Q*) (◇), SL2/*pbp5*(*5K-S*) (◆), and SL2/*pbp5*(*K199Q*) (▲).

one may conclude that the recombination events had no polar effect on the genes placed downstream of *pbp3*.

Induced SL2 cells (0.25 μg of nisin/ml) grown overnight in BHI broth supplemented with chloramphenicol were collected by centrifugation, resuspended in nisin-free medium, and used as inoculum (1%). As can be seen in Fig. 3, after a short lag period (<1 h), induced SL2 cells could multiply almost as fast as SL1 cells (~37-min and ~32-min generation times, respectively). Noninduced SL2 cells, unable to synthesize both PBP5 and PBP3, did not divide for about 8 h before they resumed their growth at a slower rate (~70-min generation time). In Fig. 3, all the samples were plated in the presence of nisin, but when they were plated onto nisin-free medium, during about the first 7 h of the lag, the cells of the inoculum (~5×10^6 cells/ml) needed at least 5 days to form colonies. The number of cells capable to produce colonies after only 1 day then progressively increased (results not shown). It is important that when subcultured in nisin-free liquid medium, cells collected after regrowth in the absence of nisin grew without going through a long lag period.

Complementation of the PBP3 deficiency in SL2 by PBP5. (i) Complementation by PBP5 of *E. hirae*. SL2 cells were transformed with pDML1627 bearing the $pbp5_{Eh}$ gene to assess the complementation activity of PBP5 when PBP3 was not produced in noninduced SL2 cells. Chloramphenicol and erythromycin were always present in the medium, and noninduced SL2/pDML1627 cells designated below as SL2/$pbp5_{Eh}$ (culture grown overnight) were used as inoculum (1%). As can be seen in Fig. 3, noninduced and induced SL2/$pbp5_{Eh}$ cells had slightly longer lag periods than induced SL2 cells. However, induced SL2/$pbp5_{Eh}$ cells multiplied more rapidly than noninduced SL2/$pbp5_{Eh}$ and induced SL2 cells (~27-min and ~38-min generation times, respectively). Thus, by producing PBP5, induced (producing PBP3) or noninduced (not producing PBP3) SL2/$pbp5_{Eh}$ cells behaved much more like SL1 and ATCC 9790 cells than like noninduced SL2 (PBP3-deficient) cells.

PBP profiles of radioactively labeled membranes of noninduced SL2 and noninduced and induced SL2/$pbp5_{Eh}$ cells were compared with those of membranes of the wild-type strain, the PenG-resistant R40 strain, and the SL1 and induced SL2 strains. It is worth noticing that the noninduced SL2 cells, collected during the growth phase that followed the 8-h lag period, produced as much PBP3 as the ATCC 9790, R40, SL1, and SL2/$pbp5_{Eh}$ cells used as controls (Fig. 4A). Obviously, in those noninduced SL2 cells, expression of the *pbp3* gene was, for unknown reasons, made possible again.

It is important that noninduced SL2/$pbp5_{Eh}$ cells produced PBP5 but not PBP3 (Fig. 4A and B). When nisin was present, the same cells produced PBP3 at the same time as PBP5. In

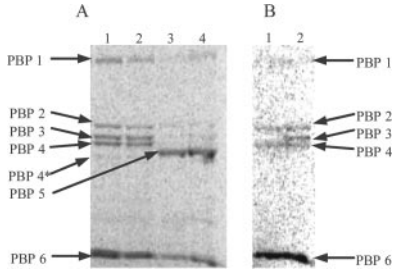

FIG. 4. SDS-PAGE and fluorogram of the membrane-bound $PBP5_{Eh}$ of *E. hirae* SL2 cells expressing $pbp5_{Eh}$ variants. (A) Membranes were labeled for 60 min with 100 μM [^{14}C]PenG. Lane 1, noninduced SL2; lane 2, induced SL2; lane 3, noninduced SL2/$pbp5_{Eh}$; lane 4, induced SL2/$pbp5_{Eh}$. (B) Membranes were labeled for 10 min with 10 μM [^{14}C]PenG. Lane 1, noninduced SL2/$pbp5_{Eh}$; lane 2, induced SL2/$pbp5_{Eh}$. Under these conditions, labeling of $PBP5_{Eh}$ is generally low.

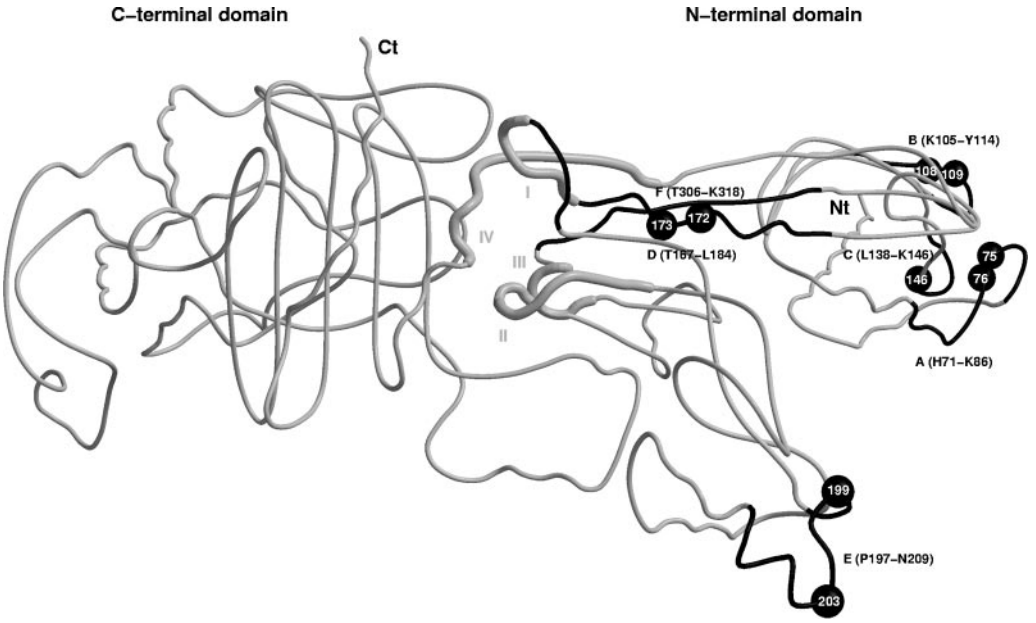

FIG. 5. Model presenting the principal putative protein-protein interaction sites identified in the N-terminal module of the PBP5 structure extending from residues 39 to 353 (53). Conserved motifs of class B PBPs are shown as the thickened gray segments (roman numerals). The sequences and the positions of the predicted interaction sites are represented by letters and black segments. The numbers and positions of substituted amino acids are indicated by black circles. Nt and Ct, N and C termini.

both cases, the amount of PBP5 was apparently similar. One can conclude that, in contrast to the noninduced SL2 cells collected after the 8-h latent period, in the SL2/*pbp5*$_{Eh}$ cells, the *nisAp* promoter was not activated. One may thus conclude that when PBP5 is produced in these cells, it is able to replace PBP3.

(ii) Complementation by PBP5 of *E. faecium*. As the PBP5 of *E. faecium* (PBP5$_{Efm}$) was shown to be closely related (80% identity) to that of *E. hirae* (PBP5$_{Eh}$) (67), both proteins were compared for their complementation activity in noninduced SL2 cells. An S_{422}A PBP5$_{Efm}$ [PBP5$_{Efm}$(S422A)] mutant, unable to bind [^{14}C]PenG and used as a control in binding experiments, was included in the assay to confirm that the DD-peptidase activity was essential for complementation.

Two shuttle plasmids, pDML2330 (*pbp5*$_{Efm}$) and pDML2331 [*pbp5*$_{Efm}$(*S422A*)], analogous to those described above to produce PBP5, were used to complement SL2 cells. Production of the PBP5$_{Efm}$ variants was verified by Western blot analysis (data not shown). Nisin-induced SL2/*pbp5*$_{Efm}$ and SL2/*pbp5*$_{Efm}$(*S422A*) cells grew at almost the same rate (~40-min generation time) but slower than induced SL2/*pbp5*$_{Eh}$ cells (~27-min generation time). PBP5$_{Efm}$ could complement the PBP3 deficiency but apparently not to the same extent as PBP5$_{Eh}$. Noninduced SL2/*pbp5*$_{Efm}$ cells indeed multiplied at a slower rate (~60-min generation time) than SL2/*pbp5*$_{Eh}$ cells (~38-min generation time). The PBP5$_{Efm}$ mutant synthesized in those noninduced cells did not help them to recover their division processes. Their growth curves were not different from those of noninduced SL2 cells with an ~8-h latent phase preceding slow growth.

In conclusion, PBP5$_{Efm}$ is able to rescue cells that do not synthesize PBP3 but apparently with a lower efficiency than its ortholog. It is also clear that for that compensatory activity, PBP5$_{Efm}$ needs to have a functional DD-peptidase module.

Identification of putative protein-protein interaction sites in the N-terminal module. Because of its very high identity with PBP5$_{Efm}$ (67), PBP5$_{Eh}$ should have a three-dimensional structure very similar to that established for PBP5$_{Ef}$ (Fig. 5) (53). Calculation of <H> and <μ> values based on the primary structure of PBP5$_{Eh}$ led to the identification of six segments that were positioned in the N-terminal module made of a long and narrow β-sheet formed by three strands and bearing two small globular domains (Fig. 5). Site A (H_{71}SQTKKTISEKE ALEK_{86} segment), site B (K_{105}VTKKDSETY$_{114}$ segment), and site C (L_{138}TNKNDQK_{146} segment) are part of the globular N-terminal domain extending from residues 39 to 162. Site D (T_{167}SEEAKRGDILDRNGKKL_{184} segment), with the important E_{170}-I_{176} and N_{180}-K_{182} residues, overlaps the first conserved motif (motif I) characterizing class B PBPs. It extends over a large part of one of the β-strands and a turn in close contact to the C-terminal module. Site E (segment P_{197} RKLGEKEEKTAN_{209}), placed about 15 amino acids downstream of motif I, is part of the globular domain at positions 190 to 260 in the center of the N-terminal module. Finally, site F (T_{306}YDKELRGTNGGK_{318} segment) starts immediately downstream of the conserved motif III and extends over another one of the three β-strands.

On the basis of the predictive method, sites D and E appeared to be most important, and the K_{172}N and R_{173}N single and double substitutions were expected to drastically reduce the potential interacting activity of site D. A similar conclusion was reached for the K_{199}Q and K_{203}Q modifications in site E.

Expression of PBP5$_{Eh}$ mutants in *E. hirae* SL1. The different variants of pDML1626, carrying *pbp5*$_{Eh}$ or the *pbp5*$_{Eh}$

mutants, were fused to pIL253 to obtain *E. coli*/*E. hirae* shuttle vectors that were named pDML1627 (*pbp5*$_{Eh}$), pDML1628 [*pbp5*(*K172N*/*R173N*)], pDML1629 [*pbp5*(*K199Q*/*K203Q*)], pDML1630 [*pbp5*(*K203Q*)], pDML1632 [*pbp5*(*R173N*)], and pDML1633 [*pbp5*(*K199Q*)]. The additional pDML1631 [*pbp5*(*5K-S*)] construct included in this study was previously prepared for other purposes (N. Hoyez, unpublished results). It carried a mutated *pbp5*$_{Eh}$ gene that encoded the five $K_{75}S$, $K_{76}S$, $K_{108}S$, $K_{109}S$, and $K_{146}S$ substitutions located in the three first putative protein-protein interaction sites identified in PBP5$_{Eh}$ (Fig. 5). The effects of these five substitutions on the amphiphilicity of sites A, B, and C were not estimated by the predictive method.

SL1 cells were transformed separately by these different shuttle vectors and grown in BHI in the presence of erythromycin. Isolated membranes of the different SL1 transformants were labeled with [^{14}C]PenG and examined by fluorography and Western blotting. SL1 transformants harboring pDML1629 [*pbp5*(*K199Q*/*K203Q*)], pDML1630 [*pbp5*(*K203Q*)], pDML1631 [*pbp5*(*5K-S*)], and pDML1633 [*pbp5*(*K199Q*)] produced as much active PBP5$_{Eh}$ as SL1/*pbp5*$_{Eh}$ cells (Fig. 1B). These mutations had apparently no structural impact on PBP5$_{Eh}$, as the binding activities appeared to be normal. In contrast, SL1/pDML1628 and SL1/pDML1632 transformants bearing the *pbp5*(*K172N*/*R173N*) and *pbp5* (*R173N*) mutations, respectively, did not synthesize any PBP5, as it could not be detected by either radioactive labeling or Western blot analysis with anti-PBP5 antibodies. As both plasmids were reisolated from these transformants and were shown to have the expected sizes and restriction sites, one can conclude that the lack of PBP5$_{Eh}$ was not due to visible plasmid modifications. However, the sequences of these *pbp5*$_{Eh}$ mutants were not verified.

Complementation of PBP3-deficient SL2 by the mutated PBP5s. The capacity of the different PBP5$_{Eh}$ variants to complement the PBP3 deficiency in noninduced SL2 cells was analyzed in several separate experiments by growing the different transformants in liquid medium as described above. The pDML1628 [*pbp5*(*K172N*/*R173N*)] and pDML1632 [*pbp5*(*R173N*)] plasmids were not included in these assays. The growth curves were established by monitoring the absorbance or the cell counts and remained similar for each clone in the different experiments. Those shown in Fig. 3 were based on cells counts made on plates containing nisin (0.25 μg/ml).

The four *pbp5*(*K199Q*/*K203Q*), *pbp5*(*K203Q*), *pbp5*(*5K-S*), and *pbp5*(*K199Q*) mutants multiplied at rates similar to that of noninduced SL2 cells (~70 min), but they differed greatly in their lag periods. In addition, some of them reached the stationary phase much earlier than the controls. The *pbp5* (*K199Q*) and *pbp5*(*5K-S*) cells needed about 3 h to reach the exponential phase. However, the *pbp5*(*5K-S*) cells stopped growing earlier than *pbp5*(*K199Q*) cells. The *pbp5*(*K203Q*) mutant and the *pbp5*(*K199Q*/*K203Q*) double mutant had to wait more than 5 h and about 7 h respectively, before they could grow regularly. In addition, *pbp5*(*K199Q*/*K203Q*) cells reached the stationary phase earlier than the *pbp5*(*K203Q*) cells.

On the basis of these experiments, one has to conclude that these mutations reduced, sometimes to a large extent, the complementation activity of PBP5$_{Eh}$.

DISCUSSION

The natural low susceptibility of enterococci to β-lactams is attributed to the protective effect of the low-affinity PBP5 that takes over most functions of the other PBPs when they are not produced or inhibited by penicillin (22, 23, 64). This means that when the essential cell division of PBP3 is inhibited by sub-MIC concentrations of PenG and PBP5 is present, the cells continue to divide (22, 23). *E. coli* and *B. subtilis* orthologs of *E. hirae* PBP3 (10, 17) interact with other membrane proteins to form the divisome, a multiprotein synthetic machinery (21, 37, 42, 62), through specific protein-protein interactions that were recently analyzed in *E. coli* (6, 16, 31, 38, 39, 45, 47, 65). For an efficient suppletive activity, the enterococcal PBP5 is probably integrated into the divisome or in a multiprotein complex with similar functions, and it should interact with one or several other proteins there.

The substitution activity of PBP5 was first specifically examined with PBP3-conditional *E. hirae* mutants that were unable to multiply at the nonpermissive temperature unless PBP5 was produced in large quantities (8). Unfortunately, those mutants were generally obtained by chemical mutagenesis and were unstable (P. Canepari, personal communication).

Determination of the principal structural elements needed for the suppletive activity of PBP5 should be done in a known and stable genetic background. A relatively long genetic engineering process was thus undertaken to first insert the *nisRK* genes by homologous recombination into the dispensable *pbp5*$_{Eh}$ gene (SL1 strain) (23, 51) and then inactivate the essential *pbp3* gene of *E. hirae* SL1 in the presence of plasmidic copies of *pbp3* placed under the control of the *nisA* promoter (*nisAp-pbp3* gene fusion).

Examination of the SL2 strain thereby obtained revealed that under inducing conditions, it did not behave not differently than the ATCC 9790 and *pbp5*::*nisRK* SL1 strains used as controls. As expected, noninduced SL2 cells did not multiply, but after about 8 h, they regained the capacity to multiply at a slower rate than induced cells. That long lag period appeared to be the time they needed to bypass, by a unknown mechanism, the control imposed by the lack of inducer. Although the amount of PBP3 produced after that lag was comparable to that found in control cells, it was insufficient to restore a normal growth rate. The presence of mutants able to produce PBP3 among the SL2 cells of the inoculum is very unlikely. From the beginning and during most of the lag period, all the cells needed at least 5 days to form colonies. This indicated that each cell of the inoculum could survive on the plates and, after a certain time, was capable of multiplying in the absence of the inducer.

The SL2 strain was nonetheless a good tool to assess the complementation activity of PBP5$_{Eh}$. When PBP5$_{Eh}$ was synthesized, the noninduced SL2 cells grew normally in spite of the absence of PBP3. They resumed their growth as fast as the control ATCC 9790, SL1, and induced SL2 cells. If they produced native PBP5$_{Efm}$, noninduced SL2 cells grew almost as if they were complemented with its PBP5$_{Eh}$ ortholog. But if they synthesized the PBP5$_{Efm}$(S422A) variant, lacking its DD-transpeptidase activity, noninduced SL2 cells were not complemented. This confirmed that, as indicated by previous results (8, 22, 23, 51, 55, 64, 67), to complement PBP-deficient cells, PBP5$_{Eh}$ must possess a functional DD-transpeptidase module.

Predictive methods used here led to the identification of six amphiphilic peptide segments that could act as protein-protein interaction sites in the structure of PBP5 of *E. hirae*. Like the other low-affinity PBPs forming subgroup B1 PBPs, $PBP5_{Eh}$ has a 110-amino-acid polypeptide insert that appears as a globular domain at the end of the N-terminal module of $PBP5_{Efm}$ (Fig. 5) (26, 53). It contains the three first sites, sites A (H_{71}-K_{86} segment), B (K_{105}-Y_{114} segment), and C (L_{138}-K_{146} segment). Site D is a relatively long peptide (T_{167}-L_{184} segment) that possesses two critical E_{170}-I_{176} and N_{180}-K_{182} subsites. It overlaps the class B PBP conserved motif I, located on one of the strands of the β-sheet connecting the N-terminal globular domain to the C-terminal module. Site E (P_{197}-N_{209} segment) was positioned between conserved motifs I and II in a region appearing as a globular domain near the center of the N-terminal module. Finally, site F (T_{306}-K_{318} segment) is found immediately downstream of motif III on another strand of the β-sheet (26, 53).

Sites D and E, which presented the strongest interaction potential, were mutagenized to introduce single or double substitutions that were proposed to reduce or suppress protein-protein interactions. Two double mutants, $K_{172}N/R_{173}N$ (M1 mutant) and $K_{199}Q/K_{203}Q$ (M2 mutant), and three single mutants, $K_{203}Q$ (M3 mutant), $R_{173}N$ (M5 mutant), and $K_{199}Q$ (M6 mutant), were prepared. A sixth mutant (M4 mutant) was added to this list, as it possessed five lysine-to-serine replacements in the three sites identified in the globular domain at the N-terminal end of PBP5. $K_{75}S$ and $K_{76}S$ mutations were introduced into site A, $K_{108}S$ and $K_{109}S$ substitutions were made in site B, and $K_{146}S$ replacement concerned the end of site C.

The N-terminal globular domain. The Lys-to-Ser substitutions made in sites A, B, and C [*pbp5*(*5K-S*)] did not seem to interfere much with the folding of the mutated $PBP5_{Eh}$ that was overproduced in SL1 cells, as the binding of [^{14}C]PenG appeared to be similar to that of $PBP5_{Eh}$. However, these substitutions modified the complementation activity of the protein, because SL2/*pbp5*(*5K-S*) cells presented a longer lag phase and a reduced growth rate and reached the stationary phase at a much lower cell density than SL2/$pbp5_{Eh}$ cells producing $PBP5_{Eh}$. These results tended to indicate that the globular domain at the extremity of the N-terminal module is implicated in the suppletive action of $PBP5_{Eh}$.

Site D. The single $R_{173}N$ and double $K_{172}N/R_{173}N$ replacements made in site D in motif I had a very drastic impact, as the $PBP5_{Eh}$ variants were not found in *E. coli* and *E. hirae* cells grown at 37°C. One may suspect that the K172 and R173 residues are essential for the stability of the protein. The $E_{76}N$ mutation made in conserved motif I of *E. coli* PBP3 (variant 10) had a milder effect in reducing the thermostability of the protein, although in this case, the hydrophobic moment plot of the I_{74}-L_{82} segment was not modified (38). The information gained with these mutations are in good agreement with structural observations suggesting that conserved motif I in class B PBPs has a critical stabilization role in the connection between the N-terminal and C-terminal modules (53). However, as both mutants, prepared separately, were not totally resequenced, one cannot totally exclude the presence of mutations that would interfere with their transcription or transduction.

The central globular domain. Our results demonstrated that site E, predicted to be an important interaction site in the central globular domain, was indeed essential for the compensatory activity of $PBP5_{Eh}$. Contrary to $PBP5_{Eh}$, the PBP5(K199Q/K203Q) variant was unable to complement PBP3-deficient SL2 cells. Lysine 203 seemed to be much more important. Its replacement by a glutamine reduced the compensatory activity to a large extent. SL2/*pbp5*(*K203Q*) cells were delayed in their growth but not as much as SL2/*pbp5*(*K199Q*/*K203Q*) and noninduced SL2 cells. Lysine 199 appeared to be of less importance. Its replacement (K199Q) had a lower impact on the complementation activity than the K203Q substitution. Thus, both residues seem to be required for a normal activity of $PBP5_{Eh}$, and when the two are replaced, $PBP5_{Eh}$ loses its suppletive activity.

In conclusion, this work definitively demonstrates that the low-affinity $PBP5_{Eh}$ alone takes over the function of PBP3 in cell division when *E. hirae* cells are submitted to β-lactam treatment. To carry out that activity, $PBP5_{Eh}$, and probably $PBP5_{Efm}$, needs the two small globular domains that are connected to the β-sheet of its N-terminal module and must have a functional C-terminal DD-transpeptidase module.

ACKNOWLEDGMENTS

We are grateful to NIZO Food Research (Ede, The Netherlands) for the generous gift of the different pNZ vectors used in this research.

This work was supported in part by the Belgian Program of Interuniversity Poles of Attraction (PAI grant P5/33), the Fonds de la Recherche Fondamentale Collective (contract 2.4521.01), the Actions de Recherche Concertées (grant 03/08-297), and European Commission grants (COBRA contract no. LSHM-CT-2003-503335 and EURINTAFAR contract no. FP6-512138). M.L., S.H., and S.L. were fellows of the Fonds pour la Formation à la Recherche dans l'Industrie et l'Agriculture (FRIA). R.B. is a research director of the Fonds National de la Recherche Scientifique (FNRS).

REFERENCES

1. **Alaedini, A., and R. A. Day.** 1999. Identification of two penicillin-binding multienzyme complexes in *Haemophilus influenzae*. Biochem. Biophys. Res. Commun. **264:**191–195.
2. **Ausubel, F. M., R. Brant, R. E. Kingston, D. D. Moore, J. G. Seidman, J. A. Smith, and K. Struhl.** 2001. Current protocols in molecular biology. John Wiley & Sons, New York, N.Y.
3. **Bayles, K. W., E. W. Brunskill, J. J. Iandolo, L. L. Hruska, S. Huang, P. A. Pattee, B. K. Smiley, and R. E. Yasbin.** 1994. A genetic and molecular characterization of the *recA* gene from *Staphylococcus aureus*. Gene **147:** 13–20.
4. **Begg, K. J., and W. D. Donachie.** 1985. Cell shape and division in *Escherichia coli*: experiments with shape and division mutants. J. Bacteriol. **163:**615–622.
5. **Biswas, I., A. Gruss, S. D. Ehrlich, and E. Maguin.** 1993. High-efficiency gene inactivation and replacement system for gram-positive bacteria. J. Bacteriol. **175:**3628–3635.
6. **Buddelmeijer, N., and J. Beckwith.** 2002. Assembly of cell division proteins at the *E. coli* cell center. Curr. Opin. Microbiol. **5:**553–557.
7. **Canepari, P., M. M. Lleo, R. Fontana, and G. Satta.** 1986. In *Streptococcus faecium* penicillin-binding protein 5 alone is sufficient for growth at submaximal but not at maximal rate. J. Gen. Microbiol. **132:**625–631.
8. **Canepari, P., M. M. Lleo, R. Fontana, and G. Satta.** 1987. *Streptococcus faecium* mutants that are temperature sensitive for cell growth and show alterations in penicillin-binding proteins. J. Bacteriol. **169:**2432–2439.
9. **Coyette, J., J. M. Ghuysen, and R. Fontana.** 1980. The penicillin-binding proteins in *Streptococcus faecalis* ATCC 9790. Eur. J. Biochem. **110:**445–456.
10. **Coyette, J., A. Somzé, J. J. Biquet, and J. M. Ghuysen.** 1983. Function of penicillin-binding protein 3 in *Streptococcus faecium*, p. 523–529. *In* R. Hakenbeck, J. V. Höltje, and H. Labischinski (ed.), The target of penicillin. Walter de Gruyter and Co., Berlin, Germany.
11. **de Pedro, M. A., K. D. Young, J. V. Höltje, and H. Schwarz.** 2003. Branching of *Escherichia coli* cells arises from multiple sites of inert peptidoglycan. J. Bacteriol. **185:**1147–1152.
12. **de Pedro, M. A., C. G. Grünfelder, and H. Schwarz.** 2004. Restricted mobility of cell surface proteins in the polar regions of *Escherichia coli*. J. Bacteriol. **186:**2594–2602.
13. **de Ruyter, P. G., O. P. Kuipers, M. M. Beerthuyzen, I. van Alan-Boerrigter,**

and W. M. de Vos. 1996. Functional analysis of promoters in the nisin gene cluster of *Lactococcus lactis*. J. Bacteriol. **178:**3434–3439.
14. **de Ruyter, P. G., O. P. Kuipers, and W. M. de Vos.** 1996. Controlled gene expression systems in *Lactococcus lactis* with the food-grade inducer nisin. Appl. Environ. Microbiol. **62:**3662–3667.
15. **de Vos, W. M.** 1999. Gene expression systems for lactic acid bacteria. Curr. Opin. Microbiol. **2:**289–295.
16. **Di Lallo, G., M. Fagioli, D. Barionovi, P. Ghelardini, and L. Paolozzi.** 2003. Use of a two-hybrid assay to study the assembly of a complex multicomponent protein machinery: bacterial septosome differentiation. Microbiology **149:**3353–3359.
17. **Duez, C., I. Thamm, F. Sapunaric, J. Coyette, and J. M. Ghuysen.** 1998. The division and cell wall cluster of *Enterococcus hirae* S185. DNA Seq. **9:**149–161.
18. **Eisenberg, D., R. M. Weiss, and T. C. Terwilliger.** 1982. The helical hydrophobic moment: a measure of amphiphilicity of a helix. Nature **299:**371–374.
19. **Eisenberg, D., E. Schwarz, M. Komaromy, and R. Wall.** 1984. Analysis of membrane and surface protein sequences with the hydrophobic moment plot. J. Mol. Biol. **179:**125–142.
20. **El Kharroubi, A., P. Jacques, G. Piras, J. Van Beeumen, J. Coyette, and J. M. Ghuysen.** 1991. The *Enterococcus hirae* R40 penicillin-binding protein 5 and the methicillin-resistant *Staphylococcus aureus* penicillin-binding protein 2′ are similar. Biochem. J. **280:**463–469.
21. **Errington, J., R. A. Daniel, and D. J. Scheffers.** 2003. Cytokinesis in bacteria. Microbiol. Mol. Biol. Rev. **67:**52–65.
22. **Fontana, R., R. Cerini, P. Longoni, A. Grossato, and P. Canepari.** 1983. Identification of a streptococcal penicillin-binding protein that reacts very slowly with penicillin. J. Bacteriol. **155:**1343–1350.
23. **Fontana, R., A. Grossato, L. Rossi, Y. R. Chang, and G. Satta.** 1985. Transition from resistance to hypersusceptibility to β-lactam antibiotics associated with loss of a low-affinity penicillin-binding protein in a *Streptococcus faecium* mutant highly resistant to penicillin. Antimicrob. Agents Chemother. **28:**678–683.
24. **Gallet, X., B. Charloteaux, A. Thomas, and R. Brasseur.** 2000. A fast method to predict protein interaction sites from sequences. J. Mol. Biol. **302:**917–926.
25. **Giesbrecht, P., J. Wecke, and B. Reinicke.** 1976. On the morphogenesis of the cell wall of staphylococci. Int. Rev. Cytol. **44:**225–318.
26. **Goffin, C., and J. M. Ghuysen.** 1998. Multimodular penicillin-binding proteins: an enigmatic family of orthologs and paralogs. Microbiol. Mol. Biol. Rev. **62:**1079–1093.
27. **Guerout-Fleury, A. M., K. Shazand, N. Frandsen, and P. Stragier.** 1995. Antibiotic-resistance cassettes for *Bacillus subtilis*. Gene **167:**335–336.
28. **Higgins, M. L., and G. D. Shockman.** 1970. Model of cell wall growth of *Streptococcus faecalis*. J. Bacteriol. **101:**643–648.
29. **Higgins, M. L., M. Ferrero, and L. Daneo-Moore.** 1986. Relationship of shape to initiation of new sites of envelope growth in *Streptococcus faecium* cells treated with β-lactam antibiotics. J. Bacteriol. **167:**562–569.
30. **Höltje, J.** 1996. A hypothetical holoenzyme involved in the replication of the murein sacculus of *Escherichia coli*. Microbiology **142:**1911–1918.
31. **Karimova, G., N. Dautin, and D. Ladant.** 2005. Interaction network among *Escherichia coli* membrane proteins involved in cell division as revealed by bacterial two-hybrid analysis. J. Bacteriol. **187:**2233–2243.
32. **Kleerebezem, M., M. M. Beerthuyzen, E. E. Vaughan, W. M. de Vos, and O. P. Kuipers.** 1997. Controlled gene expression systems for lactic acid bacteria: transferable nisin-inducible expression cassettes for *Lactococcus*, *Leuconostoc*, and *Lactobacillus* spp. Appl. Environ. Microbiol. **63:**4581–4584.
33. **Kruse, T., J. Bork-Jensen, and K. Gerdes.** 2005. The morphogenetic MreBCD proteins of *Escherichia coli* form an essential membrane-bound complex. Mol. Microbiol. **55:**79–89.
34. **Kuipers, O. P., M. M. Beerthuyzen, P. G. de Ruyter, E. Luesink, and W. M. de Vos.** 1995. Autoregulation of nisin biosynthesis in *Lactococcus lactis* by signal transduction. J. Biol. Chem. **270:**27299–27304.
35. **Lleo, M. M., P. Canepari, and G. Satta.** 1990. Bacterial cell shape regulation: testing of additional predictions unique to the two-competing-sites models for peptidoglycan assembly and isolation of conditional rod-shaped mutants from some wild-type cocci. J. Bacteriol. **172:**3758–3771.
36. **Loureiro Dos Santos, A. L., and A. Chopin.** 1987. Shotgun cloning in *Streptococcus lactis*. FEMS Microbiol. Lett. **166:**355–360.
37. **Margolin, W.** 2000. Themes and variations in prokaryotic cell division. FEMS Microbiol. Rev. **24:**531–548.
38. **Marrec-Fairley, M., A. Piette, X. Gallet, R. Brasseur, H. Hara, C. Fraipont, J. M. Ghuysen, and M. Nguyen-Distèche.** 2000. Differential functionalities of amphiphilic peptide segments of the cell-septation penicillin-binding protein 3 of *Escherichia coli*. Mol. Microbiol. **37:**1019–1031.
39. **Mercer, K. L., and D. S. Weiss.** 2002. The *Escherichia coli* cell division protein FtsW is required to recruit its cognate transpeptidase, FtsI (PBP3), to the division site. J. Bacteriol. **184:**904–912.
40. **Mollerach, M. E., P. Partoune, J. Coyette, and J.-M. Ghuysen.** 1996. Importance of the E-46–D-160 polypeptide segment of the non-penicillin-binding module for the folding of the low-affinity, multimodular class B penicillin-binding protein 5 of *Enterococcus hirae*. J. Bacteriol. **178:**1774–1775.
41. **Morlot, C., M. Noirclerc-Savoye, A. Zapun, O. Dideberg, and T. Vernet.** 2004. The DD-carboxypeptidase PBP3 organizes the division process of *Streptococcus pneumoniae*. Mol. Microbiol. **51:**1641–1648.
42. **Nanninga, N.** 1998. Morphogenesis of *Escherichia coli*. Microbiol. Mol. Biol. Rev. **62:**110–129.
43. **Nilsen, T., A. S. Ghosh, M. B. Goldberg, and K. D. Young.** 2004. Branching sites and morphological abnormalities behave as ectopic poles in shape-defective *Escherichia coli*. Mol. Microbiol. **52:**1045–1054.
44. **Partoune, P.** 1999. PhD thesis. University of Liege, Liege, Belgium.
45. **Pastoret, S., C. Fraipont, T. Den Blaauwen, B. Wolf, M. E. G. Aarsman, A. Piette, A. Thomas, R. Brasseur, and M. Nguyen-Distèche.** 2004. Functional analysis of the cell division FtsW of *Escherichia coli*. J. Bacteriol. **186:**8370–8379.
46. **Pavan, S., P. Hols, J. Delcour, M. C. Geoffroy, C. Grangette, M. Kleerebezem, and A. Mercenier.** 2000. Adaptation of the nisin-controlled expression system in *Lactobacillus plantarum*: a tool to study in vivo biological effects. Appl. Environ. Microbiol. **66:**4427–4432.
47. **Piette, A., C. Fraipont, T. den Blaauwen, M. E. G. Aarsman, S. Pastoret, and M. Nguyen-Distèche.** 2004. Structural determinants required to target penicillin-binding protein 3 to the septum of *Escherichia coli*. J. Bacteriol. **186:**6110–6117.
48. **Pinho, M. G., and J. Errington.** 2003. Dispersed mode of *Staphylococcus aureus* cell wall synthesis in the absence of the division machinery. Mol. Microbiol. **50:**871–881.
49. **Pinho, M. G., S. R. Filipe, H. de Lancaster, and A. Tomasz.** 2001. Complementation of the essential peptidoglycan transpeptidase function of penicillin-binding protein 2 (PBP2) by the drug resistance protein PBP2a in *Staphylococcus aureus*. J. Bacteriol. **183:**6525–6531.
50. **Popham, D. L., and K. D. Young.** 2003. Role of penicillin-binding proteins in bacterial cell morphogenesis. Curr. Opin. Microbiol. **6:**594–599.
51. **Sapunaric, F., C. Franssen, P. Stefanic, A. Amoroso, O. Dardenne, and J. Coyette.** 2003. Redefining the role of *psr* in β-lactam resistance and cell autolysis of *Enterococcus hirae*. J. Bacteriol. **185:**5925–5935.
52. **Satta, G., R. Fontana, and P. Canepari.** 1994. The two-competing site (TCS) model of cell shape regulation in bacteria: the envelope as an integration point for the regulatory circuits of essential physiological events. Adv. Microb. Phys. **36:**181–245.
53. **Sauvage, E., F. Kerff, E. Fonzé, R. Herman, B. Schoot, J. P. Marquette, Y. Taburet, D. Prevost, J. Dumas, G. Léonard, P. Stefanic, J. Coyette, and P. Charlier.** 2002. The 2.4-Å crystal structure of the penicillin-resistant penicillin-binding protein PBP5fm from *Enterococcus faecium* in complex with benzylpenicillin. Cell. Mol. Life Sci. **59:**1223–1232.
54. **Scheffers, D. J., and M. G. Pinho.** 2005. Bacterial cell wall synthesis: new insights from localization studies. Microbiol. Mol. Biol. Rev. **69:**585–607.
55. **Sifaoui, F., M. Arthur, L. Rice, and L. Gutmann.** 2001. Role of penicillin-binding protein 5 in expression of ampicillin resistance and peptidoglycan structure in *Enterococcus faecium*. Antimicrob. Agents Chemother. **45:**2594–2597.
56. **Signoretto, C., M. Boaretti, and P. Canepari.** 1998. Peptidoglycan synthesis by *Enterococcus faecalis* penicillin-binding protein 5. Arch. Microbiol. **170:**185–190.
57. **Simon, D., and A. Chopin.** 1988. Construction of a vector plasmid family and its use for molecular cloning in *Streptococcus lactis*. Biochimie **70:**559–566.
58. **Simon, M. J., and R. A. Day.** 2000. Improved resolution of hydrophobic penicillin-binding proteins and their covalently linked complexes on a modified C18 reversed phase column. Anal. Lett. **33:**861–867.
59. **Spratt, B. G.** 1975. Distinct penicillin-binding proteins involved in the division elongation and shape of *Escherichia coli* K12. Proc. Natl. Acad. Sci. USA **72:**2999–3003.
60. **Tamaki, S., H. Matsuzawa, and M. Matsuhashi.** 1980. Clusters of *mrdA* and *mrdB* genes responsible for the rod shape and mecillinam sensitivity of *Escherichia coli*. J. Bacteriol. **141:**52–57.
61. **van Heijenoort, J.** 2001. Formation of the glycan chains in the synthesis of bacterial peptidoglycan. Glycobiology **11:**25R–30R.
62. **Vollmer, W., and J. V. Höltje.** 2001. Morphogenesis of *Escherichia coli*. Curr. Opin. Microbiol. **4:**625–633.
63. **Weiss, D. S., K. Pogliano, M. Carson, L. M. Guzman, C. Fraipont, M. Nguyen-Distèche, R. Losick, and J. Beckwith.** 1997. Localization of the *Escherichia coli* cell division protein FtsI (PBP3) to the division site and cell pole. Mol. Microbiol. **25:**671–681.
64. **Williamson, R., C. Le Bouguénec, L. Gutmann, and T. Horaud.** 1985. One or two low affinity penicillin-binding proteins may be responsible for the range of susceptibility of *Enterococcus faecium* to benzylpenicillin. J. Gen. Microbiol. **131:**1933–1940.
65. **Wissel, M. C., and D. S. Weiss.** 2004. Genetic analysis of the cell division protein FtsI (PBP3): amino acid substitutions that impair septal localization of FtsI and recruitment of FtsN. J. Bacteriol. **186:**490–502.
66. **Young, K. D.** 2003. Bacterial shape. Mol. Microbiol. **49:**571–580.
67. **Zorzi, W., X. Y. Zhou, O. Dardenne, J. Lamotte, D. Raze, J. Pierre, L. Gutmann, and J. Coyette.** 1996. Structure of the low-affinity penicillin-binding protein 5 PBP5fm in wild-type and highly penicillin-resistant strains of *Enterococcus faecium*. J. Bacteriol. **178:**4948–4957.